

OMAE2012-8' \$%&

WAVE EFFECTS ON VORTEX-INDUCED MOTION (VIM) OF A LARGE-VOLUME SEMI-SUBMERSIBLE PLATFORM

Rodolfo T. Gonçalves¹
(rodolfo_tg@tpn.usp.br)

Guilherme F. Rosetti¹
(guilherme.feitosa@tpn.usp.br)

André L. C. Fajarra¹
(afujarra@usp.br)

Kazuo Nishimoto¹
(knishimo@usp.br)

Allan C. Oliveira²
(allan_carre@petrobras.com.br)

¹TPN – Numerical Offshore Tank
Department of Naval Architecture and Ocean Engineering, Escola Politécnica – University of São Paulo
São Paulo, SP, Brazil

²Research and Development Center (CENPES)
Petrobras
Rio de Janeiro, RJ, Brazil

ABSTRACT

Aiming to complete the results presented before by Gonçalves *et al.* (2011) – *Experimental Study on Vortex-Induced Motions (VIM) of a Large-Volume Semi-Submersible Platform*, OMAE2011, the present work brings new experimental results on VIM of a large-volume semi-submersible platform, particularly concerning its coexistence with waves in the free surface. The VIM tests were performed in the presence of three regular waves and also three different conditions of sea state. According to the results, considerable differences between the presence of regular or irregular waves were observed. The motion amplitudes in the transverse direction decreased harshly when the regular waves were performed and no VIM was observed. In the case of sea state condition tests, the amplitudes decreased slightly but a periodic motion characterized by the VIM was observed. The results herein presented concern transverse and yaw motion amplitudes, as well as spectral analyses.

Keywords: vortex-induced motions (VIM), semi-submersible, model tests, concomitant presence of wave and current, regular waves, sea conditions

1. INTRODUCTION

As opposed to what happens with cylindrical platforms such as monocolumns and spars, the study of VIM phenomenon on semi-submersibles is quite more recent and, therefore, much less can be found about it; even so important works can be cited, among them, Rijken *et al.* (2004, 2011), Waals *et al.* (2007), Rijken & Leverette (2008), Hong *et al.* (2008), Hussain *et al.* (2009), Magee *et al.* (2011) and Tahar & Finn (2011). Probably, it happens because this phenomenon was only noticed after the increase in size of the new semi-submersibles, mainly the dimension of their columns.

In a previous work, Gonçalves *et al.* (2011) performed a series of tests to verify the influence of the current incidence angle and the hull appendages on VIM of a semi-submersible. The main results showed that VIM in the transverse direction occurred in a range of $4.0 \leq Vr \leq 14.0$ with amplitude peaks around $7.0 \leq Vr \leq 8.0$. The largest amplitudes obtained were around 40% of the column width for 30 and 45-degree incidences. Another important result observed was a considerable yaw motion oscillation, denominated VIY – Vortex-Induced Yaw, in which a synchronization region could be identified as a resonant phenomenon. The largest yaw

motions were verified for the 0 and 180-degree incidences and the maxima amplitudes around 4.5°.

Under this context and aiming to complete the results presented before, the present work brings new experimental results on VIM of a large-volume semi-submersible platform illustrated in Figure 1, particularly as to its coexistence with waves in the free surface.

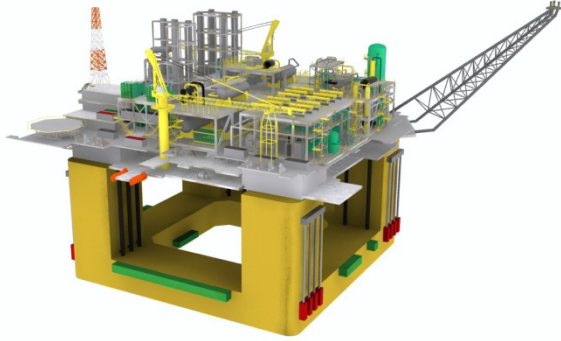


Figure 1 – Illustration of a semi-submersible with four square columns.

DNV rules (2007, 2008), discuss the effects of waves and current on the VIM. The following segment can be extracted from DNV (2008): “*VIM analysis concentrates on the effect of current. The frequencies of incoming waves are unlikely to cause vortex shedding loads in the vicinity of the low natural frequencies for sway and roll. If wind and waves are present at the same time as currents causing VIM, then they will certainly affect the system response. It seems plausible that the wave-induced fluid velocities will tend to disorganise the combined velocity field, as compared to a pure current field, and be more likely to reduce the mean amplitude of the lift force due to vortex shedding, than to increase it. Hence, it should be conservative to superimpose the forces calculated separately due to waves and vortex shedding*”. It is possible to note that is not easy to quantify these phenomena together. Another difficulty is the small number of data available about this subject in the open literature. Among the works discussing VIM together with wave effects, Dijk *et al.* (2003), Irani & Finn (2005) and Finnigan *et al.* (2005) on spar platforms; Cueva *et al.* (2006) and Gonçalves *et al.* (2010) on monocolumn platforms; and more recently, Rijken & Leverette (2008) and Hong *et al.* (2008) on semi-submersibles can be cited.

Finnigan *et al.* (2005) compared motions in the transverse direction due to current only and due to current with simultaneous wave presence on a spar platform. The waves were simulated as sea conditions with different heights. The results showed decreasing motions in the transverse direction for higher waves. Similar behavior was reported in Gonçalves *et al.* (2010) for a monocolumn platform, but with regular waves and current. The authors conjectured that the platform motion due to waves was capable of disturbing the vortex shedding implying low VIM, and if the platform motions due to

waves are small, the VIM with waves and without waves are similar.

On the other hand, Rijken & Leverette (2008) performed VIM tests of semi-submersible platforms with waves as a sea condition and conclude that the presence of waves time delayed the onset of VIM; however, similar magnitude oscillations were observed. In the same way, Hong *et al.* (2008) carried out VIM tests with waves as a sea condition, and they concluded that the wave-induced particle velocity disturbs the VIM. Even so, the data available in these tests are poor, i.e. few conditions were tested to answer the questions about wave effects.

Therefore, VIM model tests were performed in the presence of three regular waves and also three different conditions of sea state in this work. The choice was made to better understand the interaction phenomenon between current and waves on the VIM.

2. EXPERIMENTAL SETUP

The experimental setup is characterized by a small-scale model of the semi-submersible unit supported by a set of equivalent horizontal mooring, see Figure 2, in the towing tank at the Institute of Technological Research (IPT) in São Paulo, Brazil. The adopted scale was 1:100. More details about the reduced model can be found in the previous work by Gonçalves *et al.* (2011).

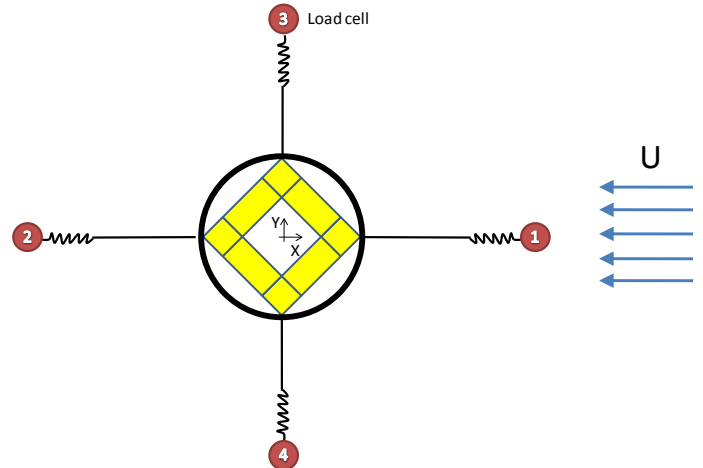


Figure 2 – Sketch of the equivalent mooring system composed of four equivalent mooring lines for 45-degree current incidence angle.

As extremely high Reynolds numbers are involved in field conditions, the usual procedure for reliable VIM tests of floating units is based on the Froude scaling, resulting in the relation:

$$Re_{model} = Re_{full} \cdot \lambda^{3/2} \quad (1)$$

where Re_{model} and Re_{full} are the Reynolds number in the model scale condition and full (field) scale one, respectively; and λ is the scale factor.

By hypothesis, the presence of a large variety of hull appendages and the geometry of semi-submersible itself are assumed to be enough to guarantee a turbulent boundary layer in subcritical regime of Reynolds number. However, the results obtained by means of this usual procedure should be considered carefully because of possible scaling effects.

The current incidence angle tested was 45 degrees, the one presenting higher VIM amplitudes in the transverse direction. At least 6 different reduced velocities were tested for each condition of coexistent wave.

The analysis methodology for defining characteristic motion amplitudes was based on a work by Gonçalves *et al.* (2012) and can be defined by taking the mean of the 10% largest amplitudes as obtained in the Hilbert-Huang Transform method (HHT), both for motion in the transverse and in-line directions, as well as for the yaw motion.

The reduced velocity is defined as

$$V_r = (U \cdot T_0) / D \quad (2)$$

where U is the incident current velocity, T_0 is the natural period of motion in the transverse direction in still water and D is the characteristic length of the cross-section of the body subjected to a vortex shedding, i.e. $D = \sqrt{2}L$ for 45-degree incidence, where L is the face dimension of the column.

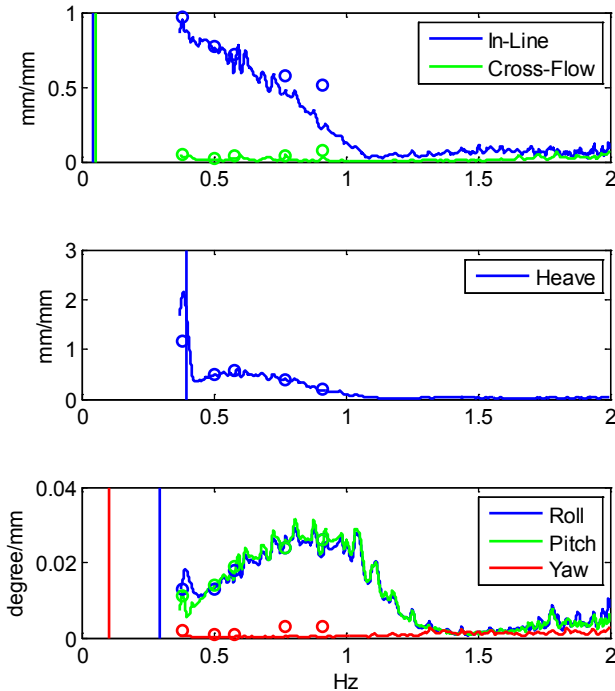


Figure 3 – RAOs for the semi-submersible with four square columns. Lines were obtained from sea condition tests and points by regular wave ones without current incidence.

Regular and irregular waves (sea conditions) were performed to verify effects coming from the presence of energy in different frequency ranges on VIM.

Three irregular waves (sea conditions) represented by a JONSWAP spectra were chosen to represent different environmental conditions at Campos Basin – Brazil, corresponding to distinct levels of unit motion. Table 2 presents the characteristic parameters of the sea conditions performed, as well as the respective power spectra in Figure 4.

Table 1 – Regular wave characteristics without current incidence.

| ID | Model scale – 1:100 | | Full scale – 1:1 | | KA |
|----|---------------------|----------|------------------|---------|------|
| | f_{RW} [Hz] | H [mm] | T_{RW} [s] | H [m] | |
| 1 | 0.91 | 43.87 | 10.99 | 4.39 | 7.3% |
| 2 | 0.59 | 78.91 | 16.95 | 7.89 | 5.5% |
| 3 | 0.38 | 116.64 | 26.32 | 11.66 | 3.4% |
| 4 | 0.77 | 54.28 | 12.99 | 5.43 | 6.5% |
| 5 | 0.50 | 81.66 | 20.00 | 8.17 | 4.1% |

Five regular waves were chosen to represent different RAO values in the heave motion; see in Figure 3 the 6 degrees-of-freedom RAO for the semi-submersible considered. This methodology was used to verify the wave effects for different vertical motion levels, as commented in Gonçalves *et al.* (2010). The regular waves performed are presented in Table 1; only the waves with ID from 1 to 3 were carried out with current incidence.

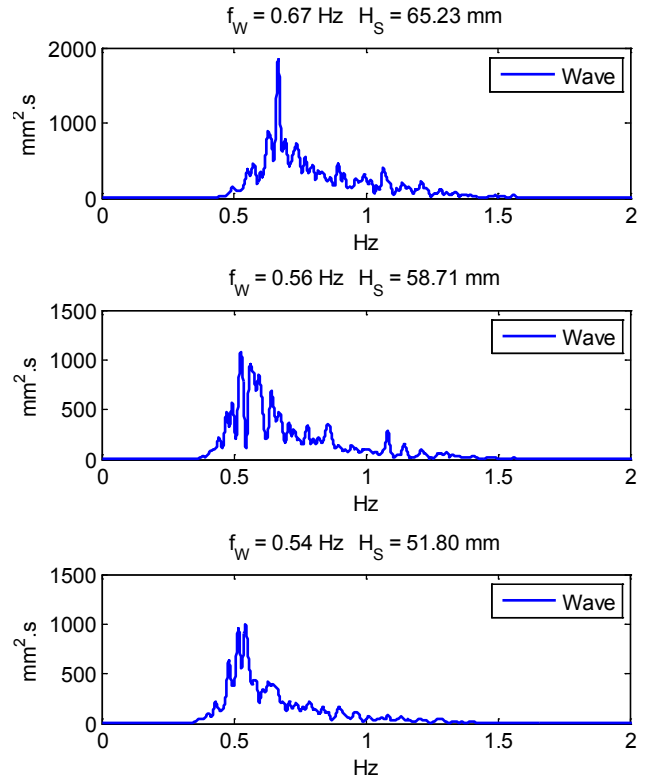


Figure 4 - PSD for JONSWAP sea conditions without current incidence: (a) $f_p = 0.67\text{Hz}$ and $H_s = 65.23\text{mm}$, (b) $f_p = 0.56\text{Hz}$ and $H_s = 58.71\text{mm}$, and (c) $f_p = 0.54\text{Hz}$ and $H_s = 51.80\text{mm}$.

Table 2 – JONSWAP sea condition characteristics without current incidence.

| ID | Model scale – 1:100 | | Full scale – 1:1 | | KA |
|----|---------------------|------------|------------------|-----------|------|
| | f_p [Hz] | H_s [mm] | T_p [s] | H_s [m] | |
| 1 | 0.67 | 65.23 | 14.93 | 6.52 | 5.9% |
| 2 | 0.56 | 58.71 | 17.80 | 5.87 | 3.7% |
| 3 | 0.54 | 51.80 | 18.62 | 5.18 | 3.0% |

Table 3 – Current velocities and respective reduced velocities performed.

| Current velocity U [cm/s] | Reduced velocity V_r |
|--------------------------------|---------------------------|
| 6.58 | 4.28 |
| 8.89 | 5.78 |
| 11.19 | 7.27 |
| 13.51 | 8.78 |
| 15.81 | 10.28 |
| 18.12 | 11.78 |

transverse VIM was observed. It is important to note that the wave encounter frequency was changed due to the current velocity; therefore, the wave encounter frequency was different for each reduced velocity. Nevertheless, these small modifications in frequency did not result in significant changes in the RAO amplitudes. More details about the natural frequency of the semi-submersible platform tested can be found in Table 4.

Table 4 – Natural frequencies in still order of the semi-submersible platform.

| Degree of freedom | Natural frequency f_N [Hz] | Natural period T_N [s] |
|-------------------|---------------------------------|-----------------------------|
| In-line | 0.04457 | 22.44 |
| Transverse | 0.05425 | 18.43 |
| Heave | 0.3973 | 2.52 |
| Roll | 0.2934 | 3.41 |
| Pitch | 0.2934 | 3.41 |
| Yaw | 0.1051 | 9.51 |

As mentioned, six current velocities were carried out to represent the main reduced velocity range in which the higher

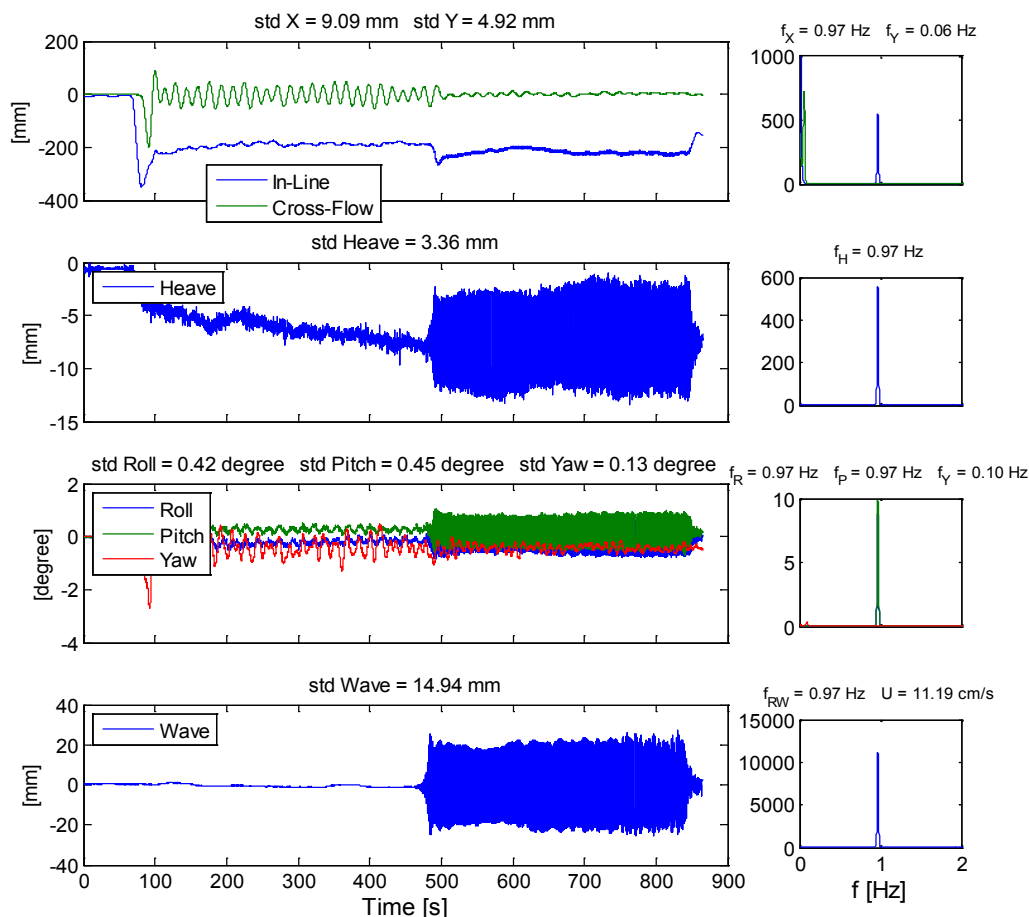


Figure 5 – Six degrees-of-freedom (in-line, transverse, heave, roll, pitch and yaw) and wave elevation for a regular wave ($f_{RW} = 0.91 \text{ Hz}$ and $H = 43.87 \text{ mm}$) and current ($U = 11.19 \text{ cm/s}$) model test time histories; and power spectrum analyses.

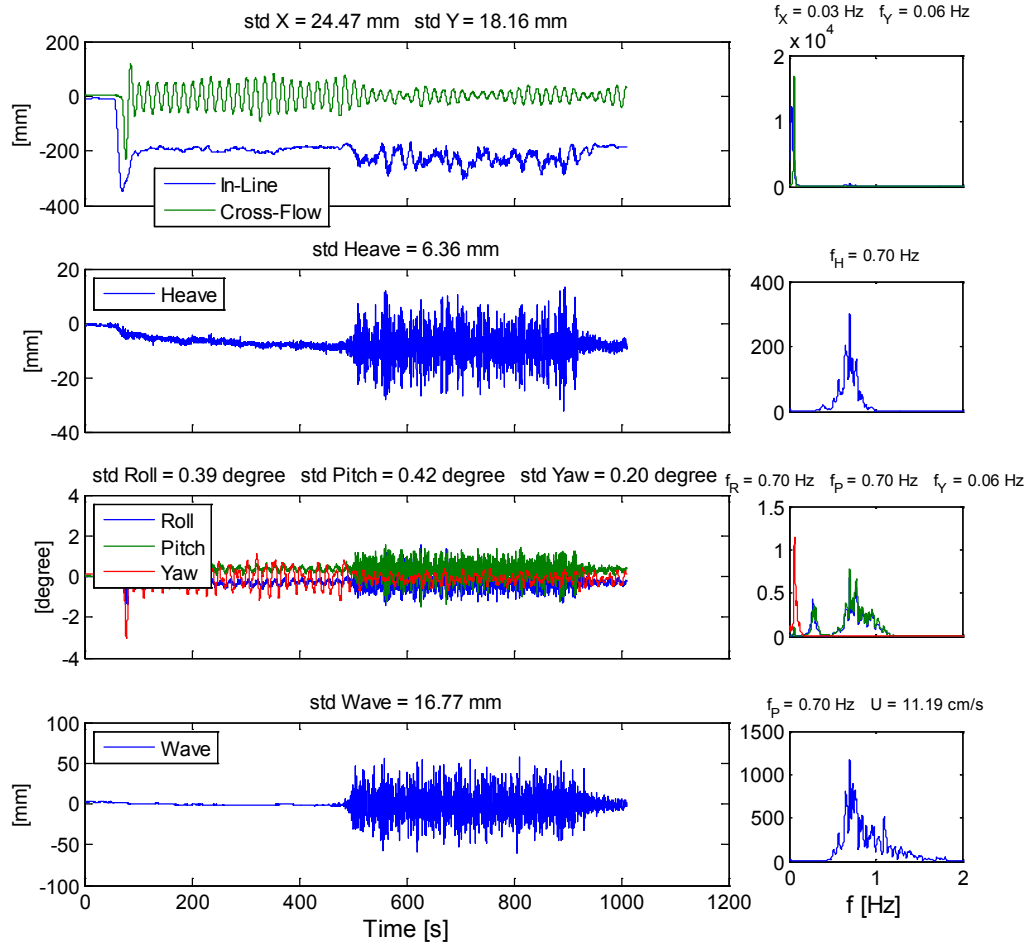


Figure 6 – Six degrees-of-freedom (in-line, transverse, heave, roll, pitch and yaw) and wave elevation for a sea condition ($f_P = 0.67\text{Hz}$ and $H_S = 65.23\text{mm}$) and current ($U = 11.19\text{cm/s}$) model test time histories; and power spectrum analyses.

Figure 5 and Figure 6 present examples of time series for a VIM test in the presence of a regular wave and a sea condition, respectively. The time histories of the 6 degree-of-freedom motions are also presented in these figures, as well the wave elevation. The first half of the test comprises only current condition incidence, where VIM is developed in steady state. Only after that the waves are performed and encountered the platform model in the last half of the test. The time along which the test is carried out with the simultaneous presence of wave and current is sufficient to observe another different steady state, and then making possible a new statistics for this range. In the same figures, power spectra are shown for each degree-of-freedom obtained for range test with wave incidence, where it is possible to verify the difference about the wave energy from regular waves (only one frequency) and sea conditions (a range of frequencies).

3. EXPERIMENTAL RESULTS

3.1. Characteristic Motion Amplitudes

Respectively, Figure 7 and Figure 8 present the results of nondimensional characteristic amplitudes for motion in the transverse direction, as well as the yaw motion amplitudes. The results are presented with and without wave presence.

According to the results in Figure 7, the motions in the transverse direction decreased with the presence of sea conditions, but the amplitudes are considerable and they have a characteristic frequency as can be further seen in Figure 13. Another issue is that the amplitudes are lower for sea conditions with higher significant amplitude. On the other hand, the VIM was mitigated completely with the presence of regular waves, and moreover the motions are similar and very low for the three regular conditions.

The results for yaw amplitudes, in Figure 8, show similar behavior, i.e. the yaw motion amplitudes decrease with the

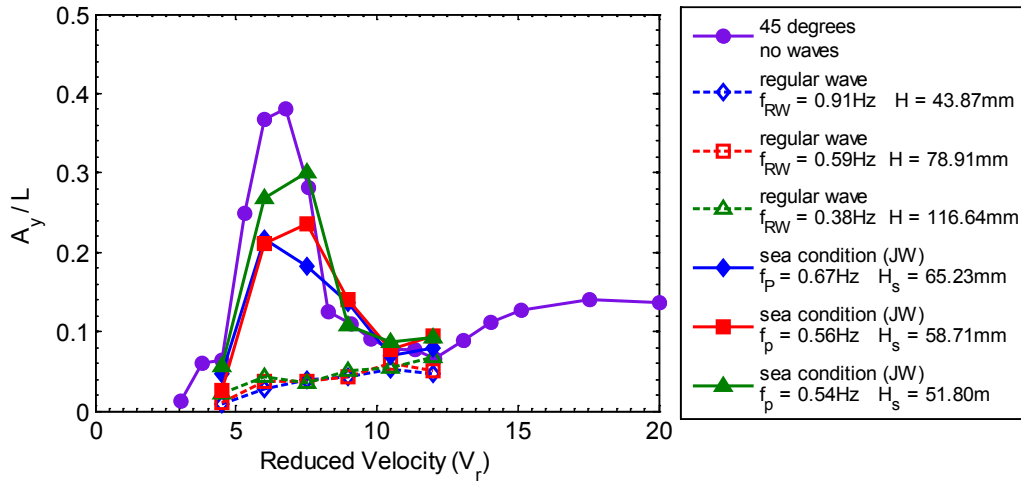


Figure 7 – Nondimensional amplitudes for the motions in the transverse direction for 45-degree current incidence: regular waves, sea conditions and without wave incidence.

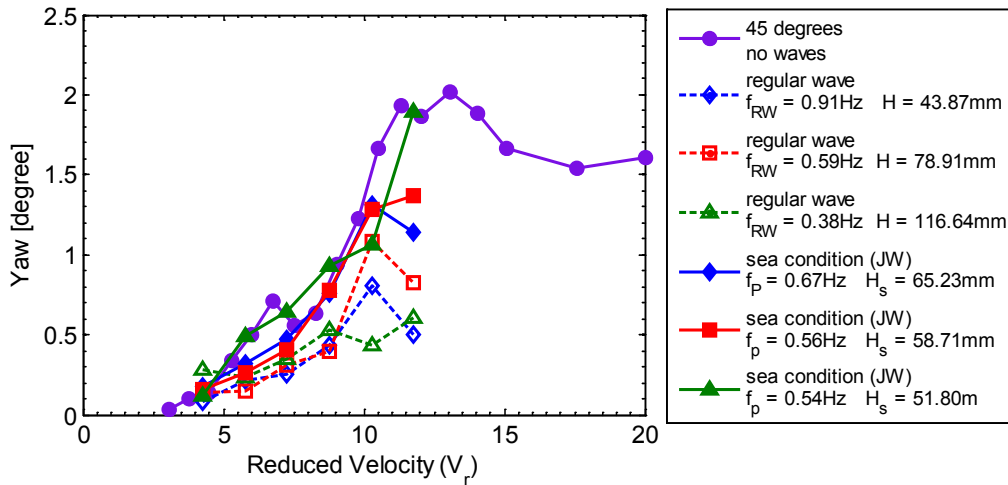


Figure 8 – Yaw characteristic amplitudes for 45-degree current incidence: regular waves, sea conditions and without wave incidence.

presence of waves and current, presenting lower amplitudes for regular wave conditions.

3.2. Power Spectrum

An important issue to be considered is the frequency analyses from Power Spectrum Density (PSD) of the motions: transverse, in-line and yaw. Figure 9 presents the PSD for 45-degree incidence without wave presence, i.e. only current incidence. The results showed no considerable energy in the in-line direction; see Figure 9a, for any frequency. However, the energy is considerable in the range of reduced velocities $5.0 \leq Vr \leq 9.0$ for the motion in the transverse direction, see Figure 9b, and in the range of reduced velocities $10.0 \leq Vr \leq 15.0$ for yaw motions, see Figure 9c. It is worth noting that the energy for transverse and yaw motion is concentrated around the natural frequency of the respective degree-of-freedom,

which corroborates the assumption that the VIM is a resonant behavior.

PSD results for the tests with the presence of waves and current are presented to better understand the wave effects on VIM, in Figures 10 to 15. Figure 10 and Figure 11 show the PSD results for the motions in the in-line direction; Figure 12 and Figure 13 for the transverse ones; and finally Figure 14 and Figure 15 for the yaw motions. The results are compared to show the different energy densities present with regular waves and sea conditions.

The greater differences between them are found in the PSD results for motions in the in-line direction. The energy for this degree-of-freedom is concentrated in the frequency of the regular waves performed, with no considerable energy in other frequencies, see Figure 10. Differently, in Figure 11, the energy density for motion in the in-line direction in the presence of sea

condition is higher and concentrated around the natural frequencies at the free surface plane (in-line and transverse, see Table 4). This behavior is known for large-volume semi-submersible, as can be seen, for example, in Matos *et al.* (2011), denominated second-order motions, which is a resonant behavior in low frequencies caused by the irregular characteristics of the sea conditions.

PSD for the motions in the transverse direction only confirms that no VIM is evidenced for regular waves; see Figure 12; and confirms the VIM behavior for sea conditions tests but with small amplitudes or small energy density around the transverse natural frequency, as seen in Figure 13.

Moreover, for the yaw motions, in Figure 14 and Figure 15, PSD results show energy density around yaw natural frequency for both wave tests, but with small energy for regular wave tests.

Taking into account the previous results, it is possible to conjecture that the resonant second-order motion in the in-line direction induced by sea condition incidence did not mitigate the VIM completely, differently from the regular wave incidence.

The VIM phenomenon has a resonant behavior as the second-order motion induced by irregular waves. Resonant phenomena are characterized by concentrated energy in the natural frequency; due to this, the VIM is not mitigated with the presence of sea conditions and thus second-order in-line motion. On the other hand, regular waves concentrate the energy in the exciting frequency, forcing system to respond in the same frequency, and not allowing it to respond around the natural frequency.

This behavior needs to be further studied, mainly through fundamental tests with cylinders subjected to current and forced to oscillate in the in-line direction simultaneously or even through cylinders free to oscillate due to a more complete set of currents and waves. This kind of investigation has been performed by the authors in other to complement the assumptions made herein.

4. GENERAL CONCLUSIONS

The VIM of semi-submersibles is an important issue to be considered in the design of risers and mooring line systems due to changes in the fatigue life of these components. Nonetheless, the VIM behavior with simultaneous presence of current and waves has not been deeply studied yet. In this context, this paper aimed to present VIM experimental results with the presence of waves: regular waves with energy distributed in a narrow range of frequency (theoretically only one frequency) and JONSWAP sea conditions, in which the energy is distributed in a range of frequencies.

The results showed that in regular wave tests the VIM was completely mitigated. Motions in the transverse direction were not observed and the energy around the natural frequency of transverse motions could not be found. Moreover, smaller yaw motion amplitudes were observed when compared with the case without wave incidences.

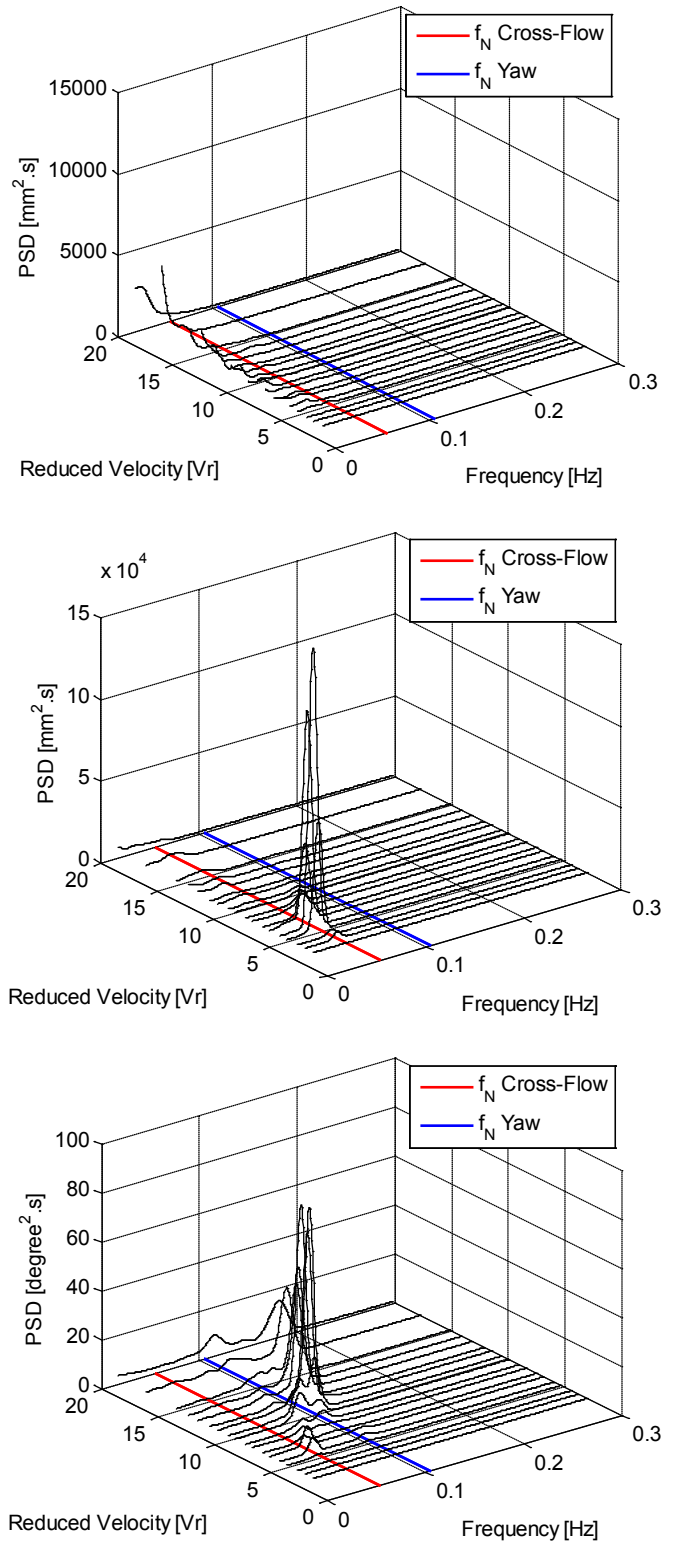


Figure 9 - PSD for 45-degree current incidence angle without waves for the motions: (a) in-line direction, (b) transverse direction, and (c) yaw.

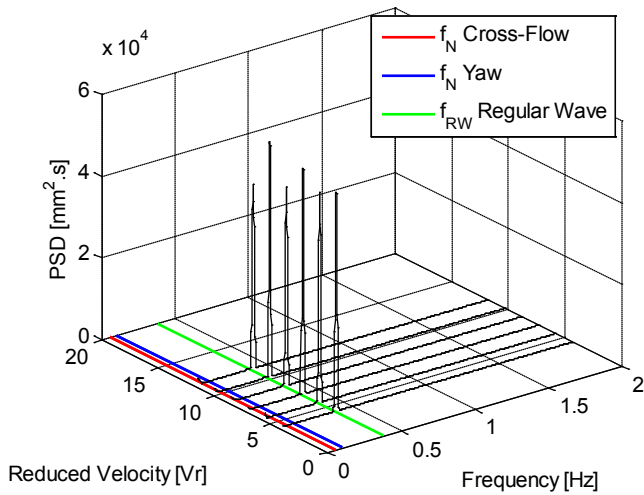
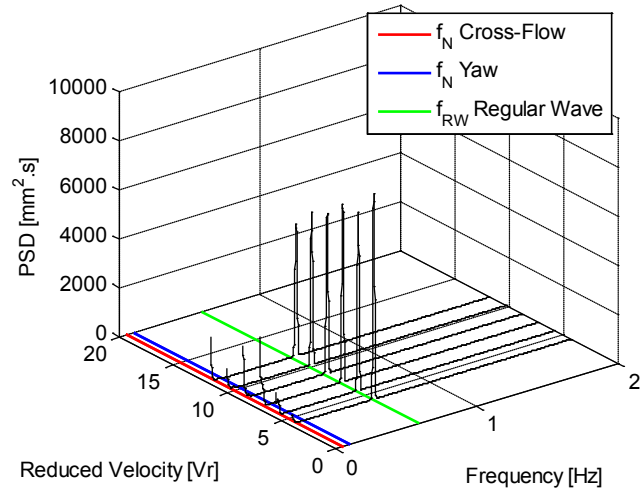
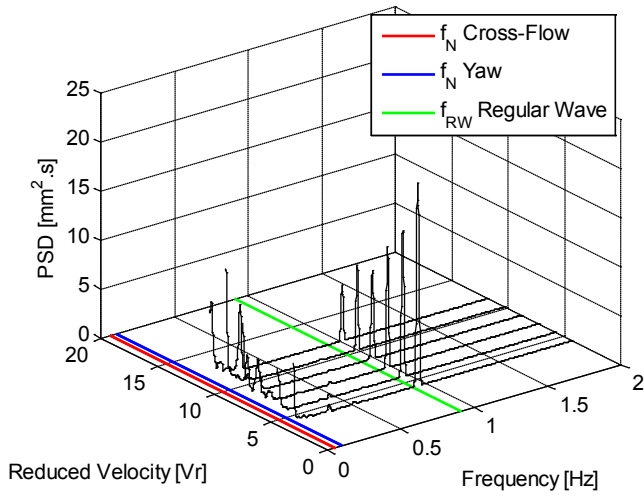


Figure 10 - PSD for the motions in the in-line direction for three different regular waves: (a) $f_{RW} = 0.91\text{Hz}$ and $H = 43.87\text{mm}$, (b) $f_{RW} = 0.59\text{Hz}$ and $H = 78.91\text{mm}$, and (c) $f_{RW} = 0.38\text{Hz}$ and $H = 116.64\text{mm}$.

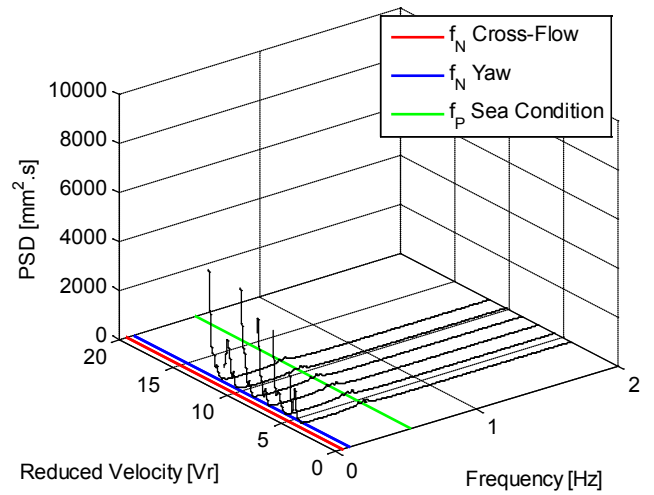
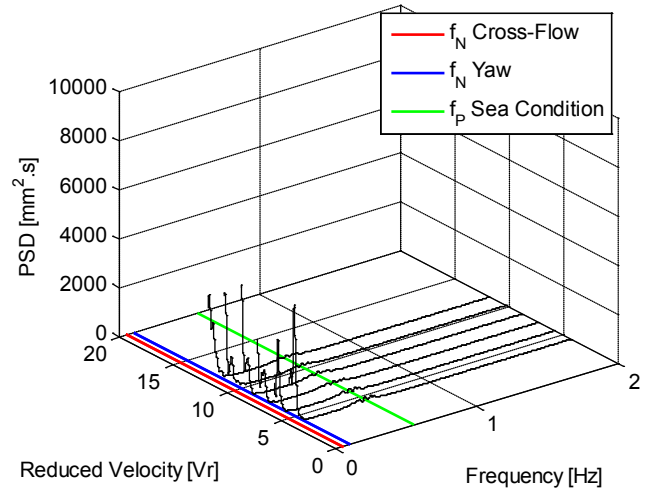
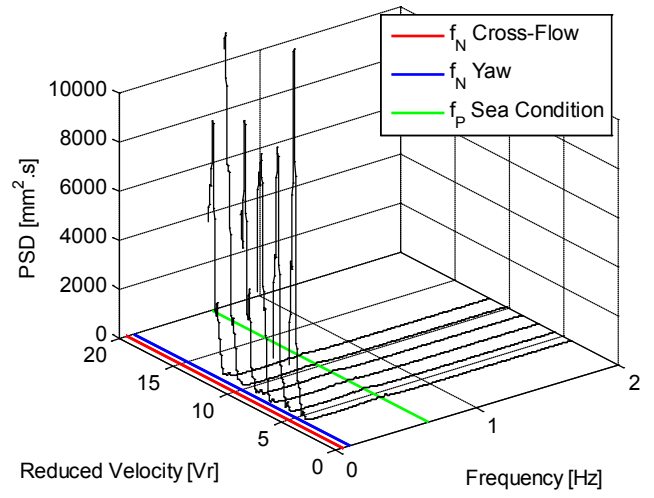


Figure 11 - PSD for the motions in the in-line direction for three different sea conditions: (a) $f_P = 0.67\text{Hz}$ and $H_S = 65.23\text{mm}$, (b) $f_P = 0.56\text{Hz}$ and $H_S = 58.71\text{mm}$, and (c) $f_P = 0.54\text{Hz}$ and $H_S = 51.80\text{mm}$.

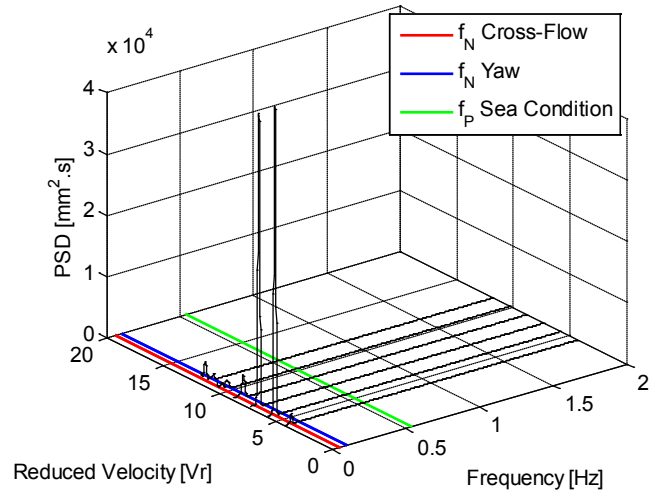
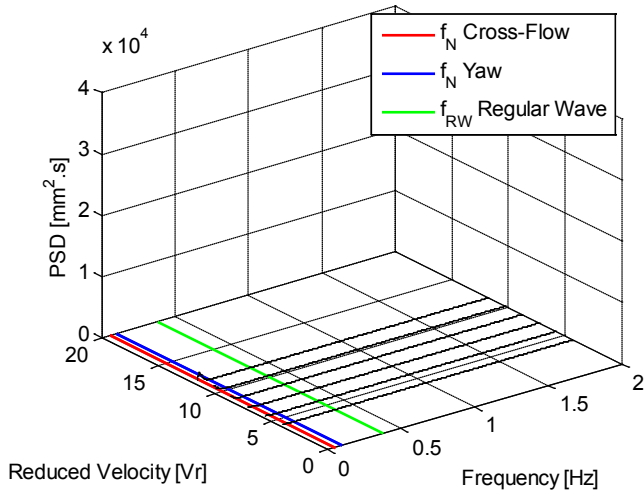
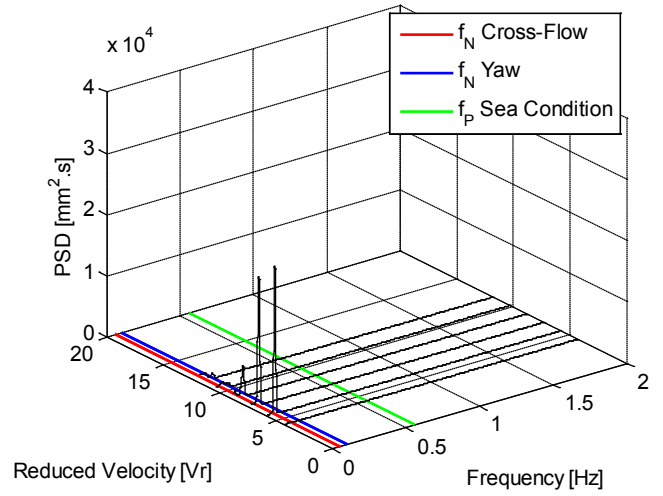
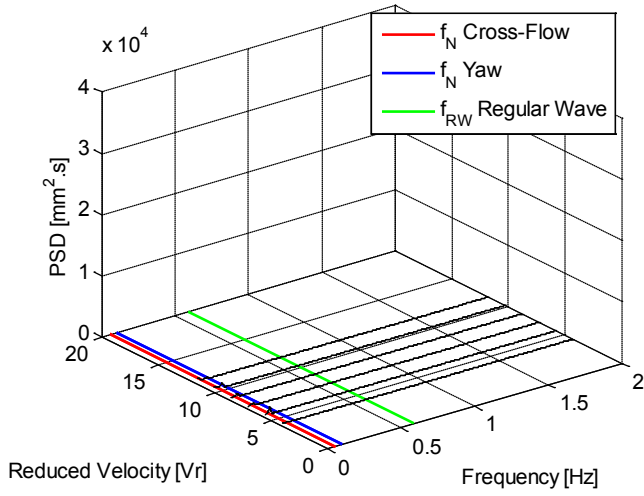
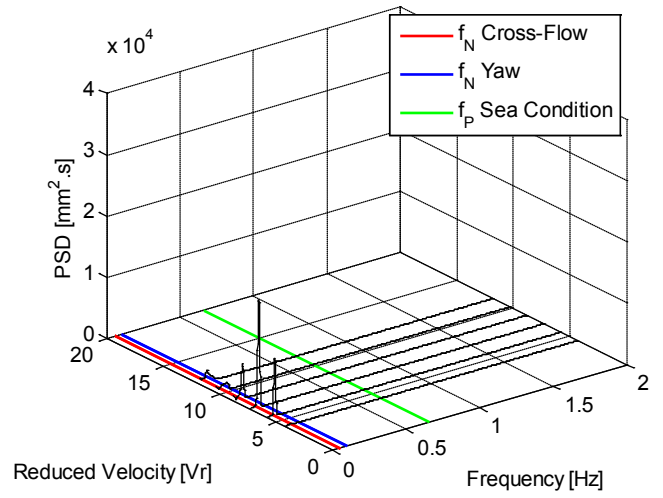
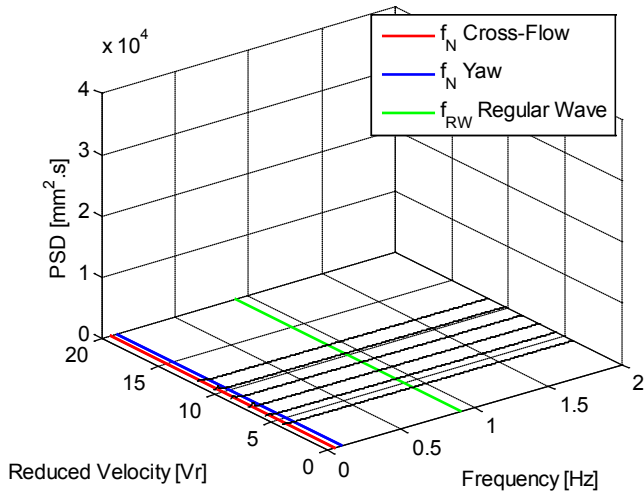


Figure 12 - PSD for the motions in the transverse direction for three different regular waves: (a) $f_{RW} = 0.91\text{Hz}$ and $H = 43.87\text{mm}$, (b) $f_{RW} = 0.59\text{Hz}$ and $H = 78.91\text{mm}$, and (c) $f_{RW} = 0.38\text{Hz}$ and $H = 116.64\text{mm}$.

Figure 13 - PSD for the motions in the transverse direction for three different sea conditions: (a) $f_p = 0.67\text{Hz}$ and $H_S = 65.23\text{mm}$, (b) $f_p = 0.56\text{Hz}$ and $H_S = 58.71\text{mm}$, and (c) $f_p = 0.54\text{Hz}$ and $H_S = 51.80\text{mm}$.

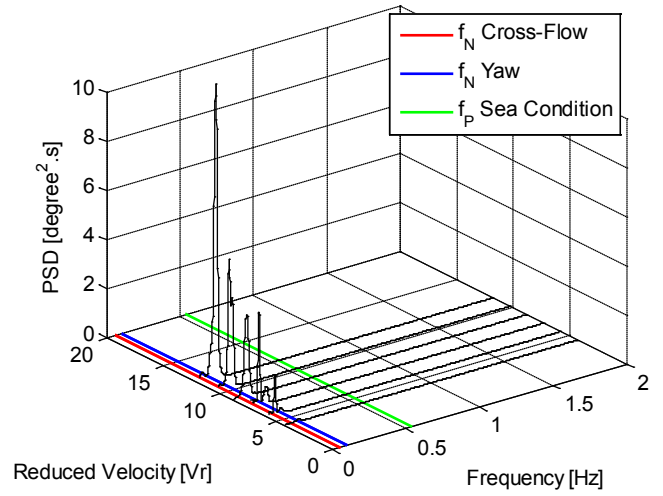
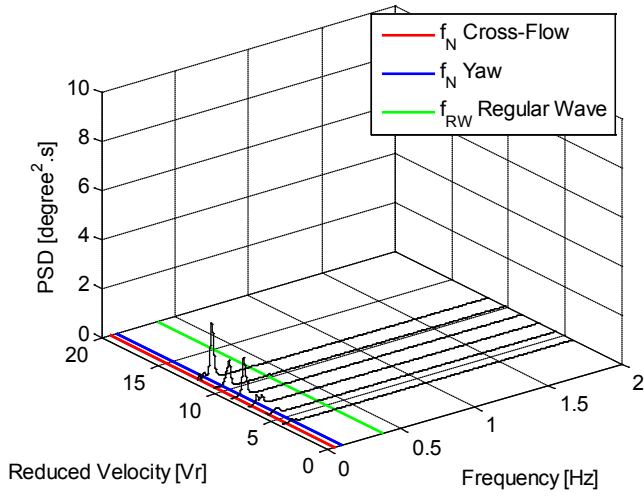
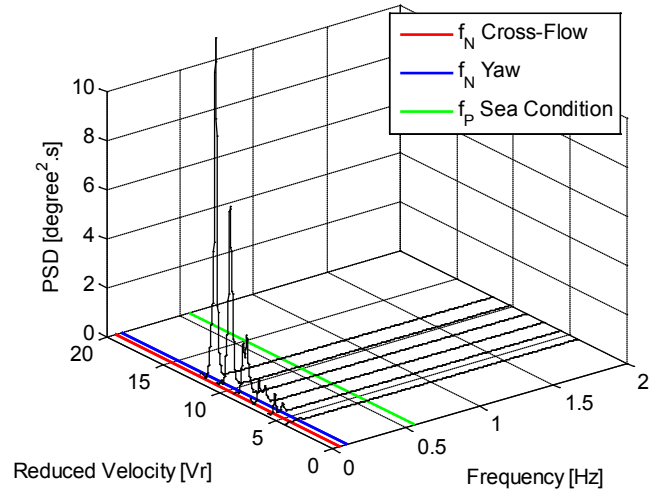
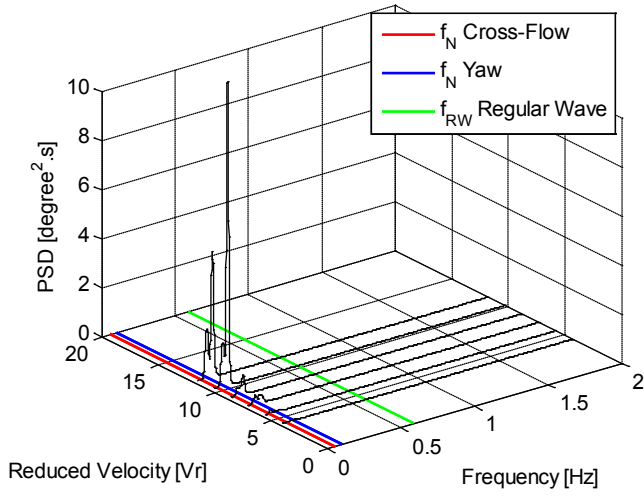
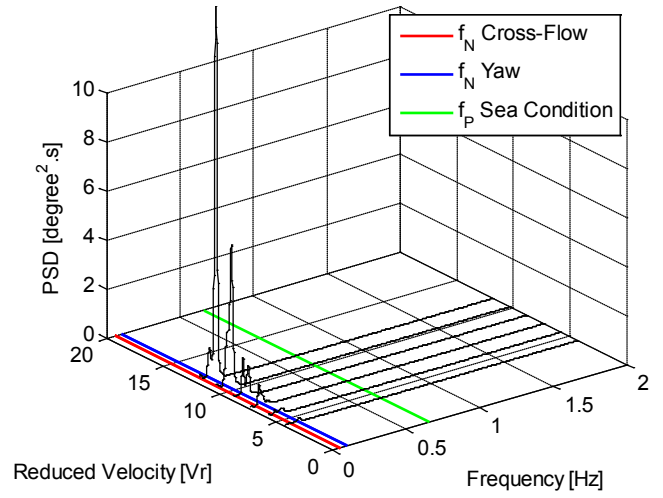
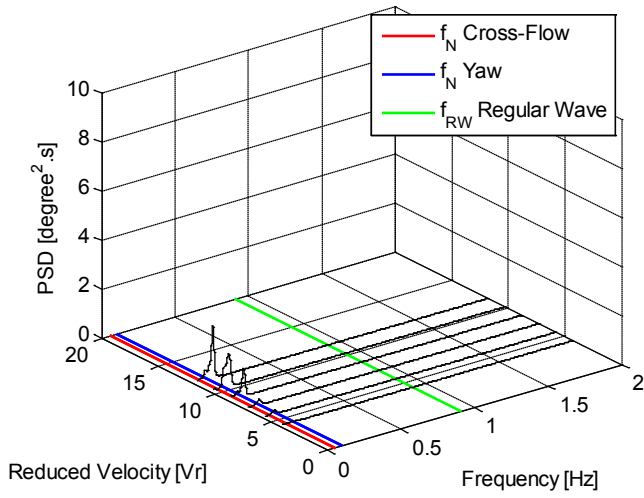


Figure 14 - PSD for yaw motions for three different regular waves: (a) $f_{RW} = 0.91\text{Hz}$ and $H = 43.87\text{mm}$, (b) $f_{RW} = 0.59\text{Hz}$ and $H = 78.91\text{mm}$, and (c) $f_{RW} = 0.38\text{Hz}$ and $H = 116.64\text{mm}$.

Figure 15 - PSD for yaw motions for three different sea conditions: (a) $f_p = 0.67\text{Hz}$ and $H_s = 65.23\text{mm}$, (b) $f_p = 0.56\text{Hz}$ and $H_s = 58.71\text{mm}$, and (c) $f_p = 0.54\text{Hz}$ and $H_s = 51.80\text{mm}$.

Differently, the results for the sea condition tests showed lower VIM when compared with the case without waves, but the PSD showed considerable energy levels around the natural frequency of motions, transverse and yaw, confirming the VIM resonant behavior.

The authors can deduce that the VIM amplitudes observed in presence of sea conditions (irregular waves) could have occurred due to the resonant second-order motion in the in-line direction, present in this type of platform. The resonant second-order motion in the in-line direction also provided energy around the natural frequency of the transverse direction, which allowed the VIM to occur. Conversely, the regular wave characteristics provided energy only in the excitation frequency, distinct from the VIM frequency, mitigating the phenomenon.

This assumption must be confirmed with more tests and deeply studied with fundamental experiments on simplified geometries such as bare cylinders, which has been made by the authors.

NOMENCLATURE

| | |
|--------------|---|
| λ | Scale factor |
| A_Y/L | Nondimensional characteristic motion amplitude in the transverse direction |
| D | Characteristic length of the section of the body subjected to a vortex shedding |
| f_N | Natural frequency in still water |
| f_P | Peak frequency |
| f_{RW} | Regular wave frequency |
| H | Regular wave height |
| H_S | Significant height |
| KA | Wave steepness |
| L | Face dimension of the column |
| Re_{full} | Reynolds number in full (field) scale |
| Re_{model} | Reynolds number in the model scale |
| T_N | Natural period |
| T_0 | Natural period of motion in the transverse direction in still water |
| T_P | Peak period |
| T_{RW} | Regular wave period |
| U | Incident current velocity |
| Vr | Reduced velocity |
| X | In-line direction |
| Y | Transverse direction |

ACKNOWLEDGMENTS

The authors thank Petrobras for their help in performing the tests. They also thank the IPT and Oceânica Offshore – Brazil personnel, in particular, Eng. MSc. Marcos Cueva, for their efforts during the test campaign. Prof. Dr. André L. C. Fajarra presents his gratitude to the Brazilian Navy and Maritime Research Institute Netherlands by the support provided during his sabbatical year, period in which this work was completed. The authors thank Prof. Dr. Celso P. Pesce for his help in the discussions. The authors would also like to acknowledge FAPESP and CAPES for the financial support.

REFERENCES

1. Cueva, M., Fajarra, A. L. C., Nishimoto, K., Quadrante, L. & Costa A. (2006) “*Vortex Induced Motion: Model Testing of a Monocolumn Floater*”. Proceedings of the 25th International Conference on Offshore Mechanics and Arctic Engineering. Hamburg, Germany. OMAE2006-92167.
2. DNV (2007). “*Recommended Practice DNV-RP-C205 – Environmental Conditions and Environmental Loads*”. April 2007.
3. DNV (2008). “*Offshore Standard DNV-OS-E301 – Position Mooring*”. October 2008.
4. Finnigan, T., Irani, M., & van Dijk, R. (2005). “*Truss SPAR VIM in Waves and Currents*”. Proceedings of the 24th International Conference on Offshore Mechanics and Arctic Engineering. Halkidiki, Greece. OMAE2005-67054
5. Gonçalves, R. T., Fajarra, A. L. C., Rosetti, G. F., & Nishimoto, K. (2010). “*Mitigation of Vortex-Induced Motion (VIM) on a Monocolumn Platform: Forces and Movements*”. Journal of Offshore Mechanics and Arctic Engineering, 132(4), p. 041102.
6. Gonçalves, R. T., Rosetti, G. F., Fajarra, A. L. C., Nishimoto, K., & Oliveira, A. C. (2011). “*Experimental Study on Vortex-Induced Motions (VIM) of a Large-Volume Semi-Submersible Platform*.” Proceedings of the 30th International Conference on Offshore Mechanics and Arctic Engineering. Rotterdam, The Netherlands. OMAE2011-49010.
7. Gonçalves, R. T., Franzini, G. R., Rosetti, G. F., Fajarra, A. L. C., & Nishimoto, K. (2012). “*Analysis Methodology for Vortex-Induced Motions (VIM) of a Monocolumn Platform Applying the Hilbert-Huang Transform Method*”. Journal of Offshore Mechanics and Arctic Engineering, Vol. 134(1), p. 011103.
8. Hong, Y., Choi, Y., Lee, J., & Kim, Y. (2008). “*Vortex-Induced Motion of a Deep-Draft Semi-Submersible in Current and Waves*”. Proceedings of the 18th International Offshore and Polar Engineering Conference. Vancouver, BC, Canada.
9. Hussain, A., Nah, E., Fu, R., & Gupta, A. (2009) “*Motion Comparison Between a Conventional Deep Draft Semi-Submersible and a Dry Tree Semi-Submersible*”, Proceedings of the 28th International Conference on Ocean, Offshore and Arctic Engineering. Honolulu, Hawaii, USA. OMAE2009-80006.
10. Irani, M. & Finn, L. (2005) “*Improved Strake Design for Vortex Induced Motions of Spar Platforms*”. Proceedings of the 24th International Conference on Offshore Mechanics and Arctic Engineering. Halkidiki, Greece. OMAE2005-67384.
11. Magee, A., Sheikh, R., Guan, K. Y. H., Choo, J. T. H., Malik, A. M. A., Ghani, M. P. A., & Abyn, H. (2011). “*Model Tests for VIM of Multi-Column Floating*

- Platforms*". Proceedings of the 29th International Conference on Ocean, Offshore and Arctic Engineering. Rotterdam, The Netherlands. OMAE2011-49151.
12. Matos, V. L. F., Simos, A. N., & Sphaier, S. H. (2011). "*Second-order resonant heave, roll and pitch motions of a deep-draft semi-submersible: Theoretical and experimental results*". Ocean Engineering, Vol. 38, pp. 2227-2243.
 13. Rijken, O., Leverette, S., & Davies, K. (2004). "*Vortex Induced Motions of Semi Submersible with Four Square Columns*". Proceedings of the 16th Deep Offshore Technology Conference and Exhibition. New Orleans, Louisiana, USA.
 14. Rijken, O., & Leverette, S. (2008). "*Experimental Study into Vortex Induced Motion Response of Semi Submersible with Square Columns*". Proceedings of the 27th International Conference on Offshore Mechanics and Arctic Engineering. Estoril, Portugal. OMAE2008-57396.
 15. Rijken, O., Schuurmans, S. & Leverette, S. (2011). "*Experimental Investigation into the Influences of SCRs and Appurtenances on Deepdraft Semisubmersible Vortex Induced Motion Response*". Proceedings of the 30th International Conference on Ocean, Offshore and Arctic Engineering. Rotterdam, The Netherlands. OMAE2011-49365.
 16. Tahar, A., & Finn, L. (2011). "*Vortex Induced Motion (VIM) Performance of the Multi Column Floater (MCF) – Drilling and Production Unit*". Proceedings of the 29th International Conference on Ocean, Offshore and Arctic Engineering. Rotterdam, The Netherlands. OMAE2011-50347.
 17. van Dijk, R. R., Magee, A., Perryman, S., & Gebara, J. (2003). "*Model Test Experience on Vortex Induced Vibrations of Truss Spars*". Proceedings of the Offshore Technology Conference (OTC 2003), Houston, USA. OTC2003-15242.
 18. Waals, O. J., Phadke, A. C., & Bultema, S. (2007). "*Flow Induced Motions of Multi Column Floaters*". Proceedings of the 26th International Conference on Offshore Mechanics and Arctic Engineering. San Diego, California, USA. OMAE2007-29539..